**Supplementary Information File**

# Probing layered Y(*TM*)$B_4$ (*TM* = Cr, Mo and W) borides as efficient hydrogen evolution reaction electrocatalysts

MD Ali Hossain[1], Lesly Delgado[1], Rutva Joshi[1], Sylvie Rangan[2], Georgiy Akopov[1,*]

[1] Department of Chemistry, Rutgers University - Newark, Newark, NJ 07102, United States.

[2] Department of Physics and Astronomy and Laboratory for Surface Modification, Rutgers University – New Brunswick, Piscataway, NJ 08854, United States

*Corresponding author: georgiy.akopov@rutgers.edu

# Table of contents

## Materials Used

Yttrium (powder, 99.9%), molybdenum (powder, 99.95%), boron (powder, 98%), tungsten (powder, 99.9%), and chromium (powder, 99%) were purchased from STREM Chemicals Inc. 20% Pt/C powder, Carbon Cloth (Sigracet), and Nafion solution were purchased from Fuel Cell Store. Sulfuric acid ($H_2SO_4$, 98%) was purchased from PHARMACO-AAPER. Epoxy resin and hardener for electrode preparation were purchased from Allied High Tech Products, Inc. All the chemicals were used without further purification.

## Experimental Section

### Synthesis Method

Ingots of Y(*TM*)$B_4$ (*TM* = Cr, Mo and W) were prepared using the following procedure. Powders of yttrium (Y), molybdenum (Mo), chromium (Cr), tungsten (W), and boron (B) were accurately weighed in the Y : (*TM*) : B = 1 : 1 :4.25 ratios (excess boron was used to account for its evaporation during arc melting) with a total mass of 0.75 g and pressed into pellets under a force of 10 tons using a hydraulic press (Carver). These pellets were then arc-melted on top of a water-cooled copper hearth, under an argon atmosphere using a tungsten tip as the electrode. Zirconium metal getters were used to ensure no presence of oxygen in the chamber. The arc current was maintained at 140 A, and the samples were turned over and remelted four times to ensure uniform composition.

### Powder X-ray diffraction (PXRD)

Powder X-ray diffraction (PXRD) analysis was carried out using a Rigaku Miniflex 600 diffractometer with Cu-Kα radiation (λ = 1.5434 Å). Zero-background silicon plates were used as sample holders. The finely ground powder samples were evenly spread onto circular holders and gently pressed with a glass slide to ensure they remained in place. During data acquisition, the sample holders were rotated at a speed of 15 rpm to improve measurement accuracy.

### XPS

X-ray photoemission spectroscopy (XPS) was conducted on a Thermo K-Alpha instrument using a monochromatized Al Kα line, and with an overall energy resolution for core levels of 0.6 eV. A flooding source was used on all samples and the C 1s (C-C) was found at 284.7 eV (+/- 0.2 eV).

Starting materials were measured under powder form, while the reacted electrode was measured after electrocatalysis.

**SEM-EDS**

The Surface morphology and mapping (point analysis) were obtained using an ultra-high-resolution field-emission scanning electron microscope (Hitachi S-4800) equipped with an EDS detector from EDAX.

**Electrochemical Characterization**

Electrochemical measurements were carried out using a Gamry Interface 1010E in a standard three-electrode configuration (Gamry Instruments Inc.). A saturated calomel electrode (SCE) was used as the reference electrode, a graphite rod as the counter electrode, and 0.5 M $H_2SO_4$ was used as the electrolyte at room temperature. A copper wire was attached to the arc-melted samples using conductive silver paste and vacuum dried at 150 °C for 1.5 hr. After the vacuum drying, samples were put into a plastic vial with epoxy glue (10 : 1 = resin : hardener ratio) and dried at room temperature for 24 hr. Then the electrode was polished with sandpaper prior to use, and surface area measurements were taken. Surface area was measured using an optical microscope. The Schematic of Electrode Preparation is given in **Figure S1**.

For the 20% Pt/C electrode, the above-mentioned procedures were carried out after the following steps: 1 mg of commercial 20% Pt/C catalyst was ultrasonically dispersed in 95 µL of ethanol and 5 µL of Nafion solution (Fuel Cell Store) for 30 minutes to obtain a uniform slurry. Then 10 µL of the resulting suspension was drop-coated onto a carbon cloth (Sigracet) with an approximate area of 0.3 × 0.3 $cm^2$. The coated electrode was then dried at 70 °C for 2 hours in a vacuum furnace to evaporate the solvent and enhance adhesion. Then, a copper wire was attached to the Pt/C support using conductive silver paste and vacuum dried at 150 °C for 1.5 hr. After the vacuum drying, samples were put into a plastic vial with epoxy glue (10 : 1 = resin : hardener ratio) and dried at room temperature for 24 hr. The loading on the Pt/C electrode was approximately 1.1 mg/$cm^2$. For the electrodes made from powder, 5 mg of synthesized arc-melted powders was ultrasonically dispersed in 75 µL of ethanol and 25 µL of Nafion solution (Fuel Cell Store) for 60 minutes to obtain a uniform slurry. Then, 10 µL of the resulting suspension was drop-coated onto a Graphite Disk Electrode (Stony Lab) with an approximate area of 0.07 $cm^2$ followed by overnight drying.

Linear sweep voltammetry (LSV) was employed to obtain polarization curves in the potential range from -1.0 V to 0.0 V vs RHE at a scan rate of 5 mV/s. Catalyst stability was measured by cyclic voltammetry (CV), at a scan rate of 100 mV/s over 5000 cycles.

All recorded potentials were converted to values versus the reversible hydrogen electrode (RHE) using $E_{RHE} = E_{SCE} + 0.241V + 0.059 \times pH$ and iR-drop compensation (iRΩ) was applied to correct solution resistance.

The electrochemically active surface area (ECSA) was determined from CV scans performed at scan rates ranging from 80 to 200 mV/s within the non-faradaic region (0.05–0.15 V vs. RHE). The double-layer capacitance ($C_{dl}$) was obtained by plotting the current density difference ($\Delta J = J_a - J_c$) at 0.1 V vs. RHE as a function of scan rate.

Electrochemical impedance spectroscopy (EIS) was performed over a frequency range of 1000 kHz to 1 Hz with a 5 mV AC perturbation.

**Table S1. Unit cell values, select bond lengths, and XPS and EDS composition data for $YCrB_4$, $YMoB_4$, and $YWB_4$.**

| Parameter \ Phase | $YCrB_4$ | $YMoB_4$ | $YWB_4$ |
|---|---|---|---|
| **Metal Ratio (EDS)** | Y : 1.15Cr | Y : 1.01Mo | Y : 1.12W |
| **Composition (XPS)** | $Y_{0.9}Cr_{0.4}B_4$ | $Y_{0.8}Mo_{0.9}B_4$ | $Y_{0.8}W_{0.6}B_4$ |
| **ICSD code** | 148214 | 235708 | 615702 |
| ***a* (Å)** | 5.9425(2) | 6.0284(8) | 6.0370(50) |
| ***b* (Å)** | 11.4831(4) | 11.6450(10) | 11.6600(100) |
| ***c* (Å)** | 3.4643(1) | 3.6120(4) | 3.5980(50) |
| **V (Å$^3$)** | 236.395 | 253.565 | 253.268 |
| **(B-B) (Å)** | 1.724 – 1.832 | 1.768 – 1.874 | 1.632 – 2.002 |
| **$(B\text{-}B)_{avg.}$ (Å)** | 1.780 | 1.807 | 1.818 |
| **(Y-B) (Å)** | 2.618 – 2.748 | 2.663 – 2.817 | 2.643 – 2.824 |
| **$(Y\text{-}B)_{avg.}$ (Å)** | 2.697 | 2.759 | 2.781 |
| **(*TM*-B) (Å)** | 2.267 – 2.325 | 2.362 – 2.400 | 2.295 – 2.385 |
| **$(TM\text{-}B)_{avg.}$ (Å)** | 2.294 | 2.375 | 2.342 |

**Table S2. Comparison of the overpotential for HER in this work with reference Pt electrodes reported previously.**

| Catalyst | Electrolyte | Current Density (mA/cm$^2$) | Overpotential (mV) | Reference |
|---|---|---|---|---|
| **$YWB_4$** | 0.5 M $H_2SO_4$ | 1000 | 557 | This work |
| **$YMoB_4$** | | | 582 | |
| **$YCrB_4$** | | | 696 | |
| **Pt/C 20%** | 0.5 M $H_2SO_4$ | 1000 | 742 | This work |
| **Pt/C 20%** | 0.5 M $H_2SO_4$ | 800 | 662 | [1] |
| **Pt/C 20%** | 0.5 M $H_2SO_4$ | 1000 | 837 | [2] |
| **Pt/C 20%** | 0.5 M $H_2SO_4$ | 1000 | 948 | [3] |
| **Pt/C 40%** | 0.5 M $H_2SO_4$ | 1000 | ~1120 | [4] |

**Table S3. Comparison of the overpotential for HER in this work with those reported previously for acidic and basic conditions (where applicable).**

| Catalyst | Material type | Electrolyte | Current Density ($mA/cm^2$) | Overpotential (mV) | Tafel plots (mV/dec) | Reference |
|---|---|---|---|---|---|---|
| $YWB_4$ | Ingot | 0.5 M $H_2SO_4$ | 10<br>100<br>1000 | 328<br>452<br>557 | 78.5 | This work |
| $YMoB_4$ | Ingot | 0.5 M $H_2SO_4$ | 10<br>100<br>1000 | 328<br>465<br>582 | 79.1 | This work |
| $YCrB_4$ | Ingot | 0.5 M $H_2SO_4$ | 10<br>100<br>1000 | 418<br>562<br>696 | 108.5 | This work |
| $YWB_4$ | Powder | 0.5 M $H_2SO_4$ | 1000 | 814 | - | This work |
| $YMoB_4$ | Powder | 0.5 M $H_2SO_4$ | 1000 | 899 | - | This work |
| $YCrB_4$ | Powder | 0.5 M $H_2SO_4$ | 1000 | 933 | - | This work |
| $MoB_2$ | Powder | 0.5 M $H_2SO_4$ | 2.5 | 230 | 75 | [5] |
| $Cr_{0.4}Mo_{0.6}B_2$ | Ingot | 0.5 M $H_2SO_4$ | 10<br>100<br>800 | 193<br>~275<br>~475 | 60.1 | [1] |
| $V_{0.3}Mo_{0.7}B$ | Nano-Powder | 0.5 M $H_2SO_4$ | 150<br>1000 | 212<br>452 | 55 | [2] |
| MoB | Powder | 0.5 M $H_2SO_4$ | 20 | 210 | 55 | [6] |
| $MoB_2$ | Powder | 0.5 M $H_2SO_4$ | 10 | 154 | 49 | [7] |
| $Mo_2B_4$ | Powder | 0.5 M $H_2SO_4$ | 10 | 310 | 80 | [8] |
| MoAlB | Crystal | 0.5 M $H_2SO_4$ | 10 | 301 | 68 | [9] |
| $MoS_2$ | Powder | 0.5M $H_2SO_4$ | 10 | 300 | 41 | [10] |
| $Mo_2C$ | Nano | 0.5M $H_2SO_4$ | 8 | 300 | 84 | [11] |
| MoP | Pellets | 0.5M $H_2SO_4$ | 30 | 180 | 54 | [12] |
| $WS_2$ | Nano-powder | 0.5M $H_2SO_4$ | 30 | ~330 | - | [13] |
| WP | Nano-powder | 0.5M $H_2SO_4$ | 10<br>20 | ~121<br>~140 | 30 | [14] |
| WC | Powder | 0.1M $H_2SO_4$ | 20 | 444 | - | [15] |
| $YWB_4$ | Ingot | 0.5M KOH | 100 | 535 | - | This work |
| $YMoB_4$ | Ingot | 0.5M KOH | 100 | 462 | - | This work |
| $YCrB_4$ | Ingot | 0.5M KOH | 100 | 656 | - | This work |
| $YWB_4$ | Powder | 0.5M KOH | 100 | 547 | - | This work |
| $YMoB_4$ | Powder | 0.5M KOH | 100 | 686 | - | This work |
| $YCrB_4$ | Powder | 0.5M KOH | 100 | 752 | - | This work |

| Co-B | Pellets | pH=1 | 10 | ~280 | 75 | [16] |
|---|---|---|---|---|---|---|
| **Catalyst** | **Material type** | **Electrolyte** | **Current Density ($mA/cm^2$)** | **Overpotential (mV)** | **Tafel plots (mV/dec)** | **Reference** |
| Co-B | Powder | 1M KOH | 10 | 110 | 80 | [17] |
| $FeB_2$ | Nano-powder | 1M KOH | 10 | 61 | 87.5 | [18] |

**Table S4. Binding energy (BE) for XPS data**

| Element | Spin orbit | BE (eV) | FWHM (eV) | References |
|---|---|---|---|---|
| $YCrB_4$ (Before) | $Y3d_{5/2}$ | 154.6 ($YB_x$)<br>158.1 ($Y_2O_3$) | 1.3<br>1.7 | [19] |
| | $Cr2p3_{/2}$ | 573.7 (Cr-B)<br>577.0 (Cr-O) | 1.6<br>3.4 | [20,21] |
| | B1s | 186.8 (Cr-B)<br>192.0 ($B_2O_3$) | 1.1<br>2.0 | [20,21] |
| $YMoB_4$ (Before) | $Y3d_{5/2}$ | 155.1 ($YB_x$)<br>158.4 ($Y_2O_3$) | 1.4<br>1.7 | [19] |
| | $Mo3d_{5/2}$ | 227.5 (Mo-B)<br>232.5 ($MoO_3$) | 1.7<br>2.1 | [20,21,22] |
| | B1s | 187.2 (Mo-B)<br>192.4 ($B_2O_3$) | 1.3<br>2.0 | [20,21] |
| $YWB_4$ (Before) | $Y3d_{5/2}$ | 155.1 ($YB_x$)<br>158.3 ($Y_2O_3$) | 1.4<br>1.7 | [19] |
| | $W4f_{7/2}$ | 30.7 ($WB_x$)<br>35.6 ($WO_3$) | 1.5<br>1.6 | [20,24] |
| | B1s | 187.2 ($WB_x$)<br>192.4 ($B_2O_3$) | 1.3<br>2.3 | [20,24] |
| $YCrB_4$ (After) | $Y3d_{5/2}$ | 158.0 ($Y_2O_3$) | 1.8 | [19] |
| | $Cr2p3_{/2}$ | 577.2 (Cr-O) | 2.9 | [20,21] |
| | B1s | 192.0 ($B_2O_3$) | 2.1 | [20,21] |
| $YMoB_4$ (After) | $Y3d_{5/2}$ | 158.3 ($Y_2O_3$) | 1.7 | [19] |
| | $Mo3d_{5/2}$ | 232.4 ($MoO_3$)<br>230.6 ($MoO_2$) | 1.7<br>2.0 | [20,21] |
| | B1s | 192.2 ($B_2O_3$) | 2.1 | [20,21] |
| $YWB_4$ (After) | $Y3d_{5/2}$ | 158.3 ($Y_2O_3$) | 1.8 | [19] |
| | $W4f_{7/2}$ | 35.5 ($WO_3$) | 1.6 | [20,24] |
| | B1s | 192.3 ($B_2O_3$) | 2.2 | [20,24] |

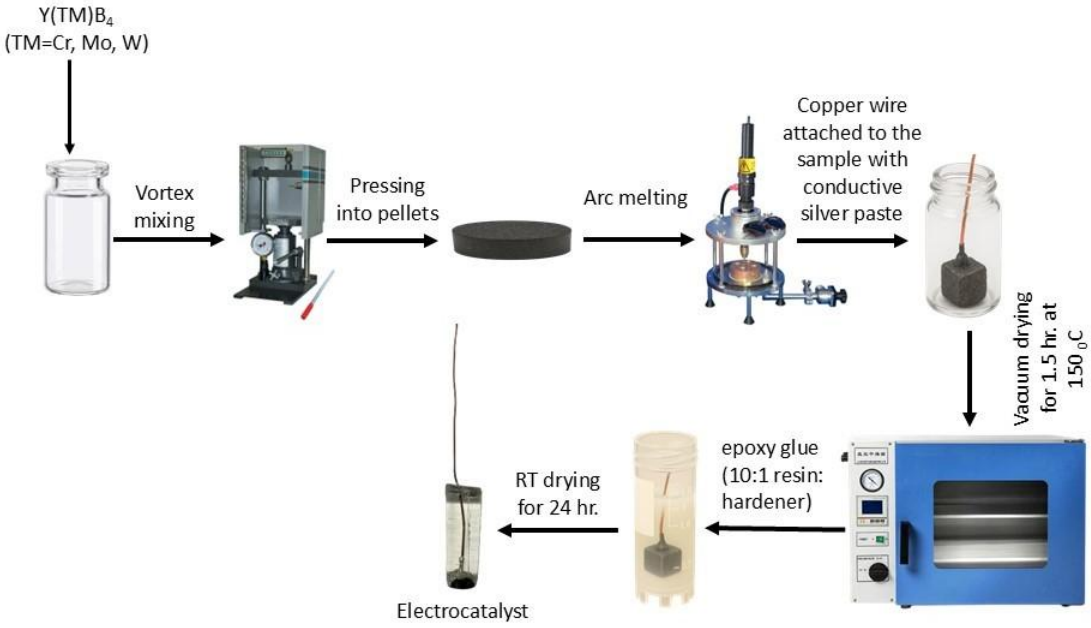


**Figure S1.** Schematic of electrode fabrication.

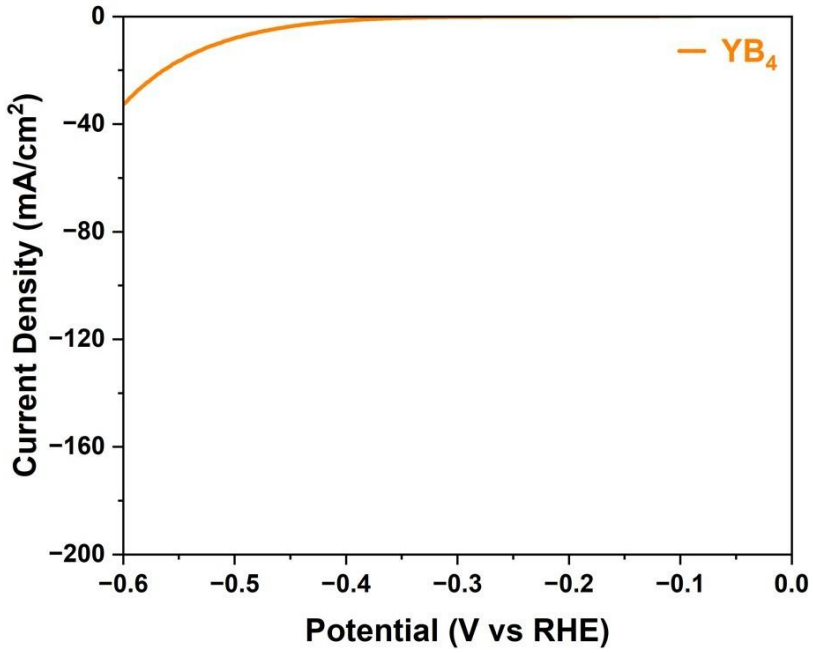


**Figure S2.** Polarization curve for $YB_4$ (impurity) phase, showing essentially no catalytic activity towards HER.

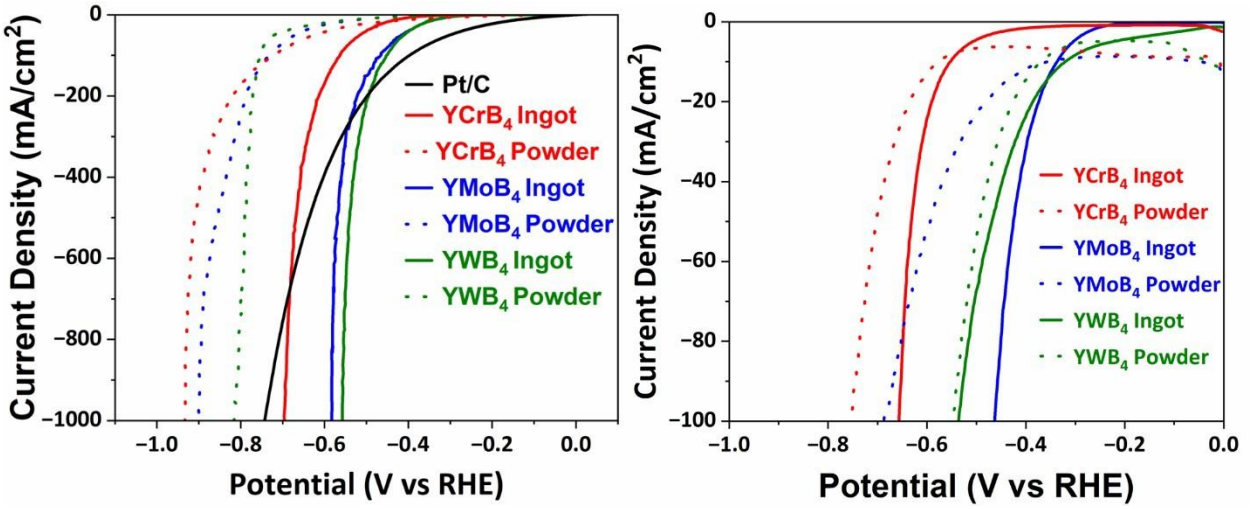


**Figure S3.** Polarization curves for $YCrB_4$, $YMoB_4$, and $YWB_4$ in both ingot and powder form measured under **(left)** acidic (0.5M $H_2SO_4$); and **(right)** basic conditions (0.5M KOH).

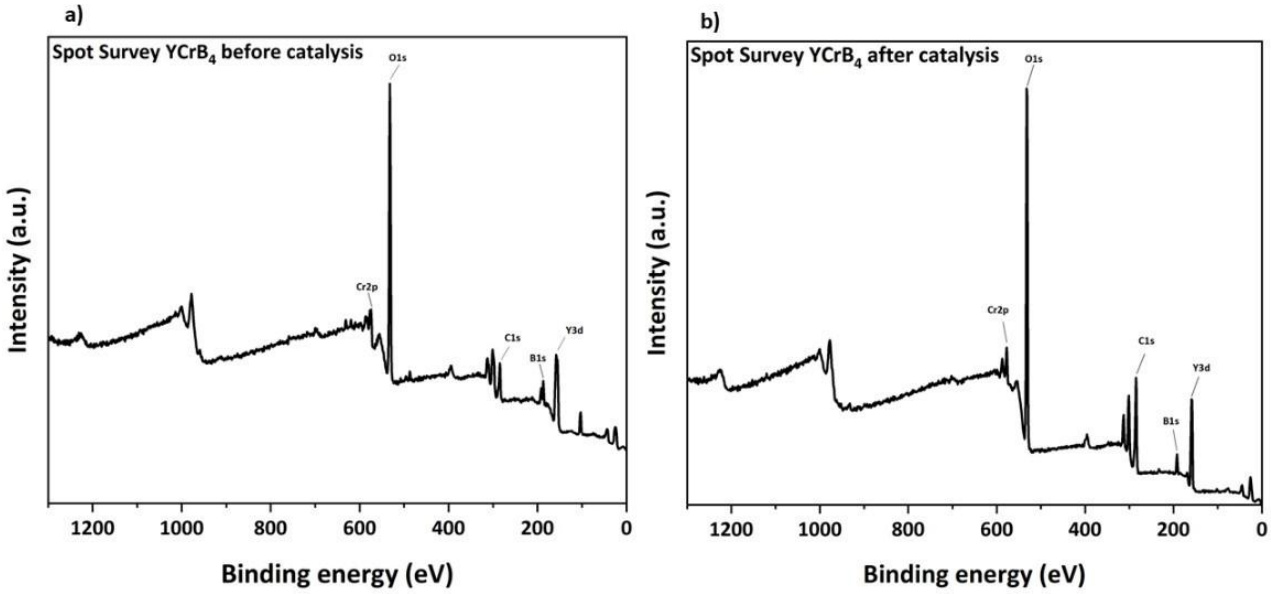


**Figure S4:** XPS survey scan for $YCrB_4$; a) Before electrocatalysis, b) After electrocatalysis

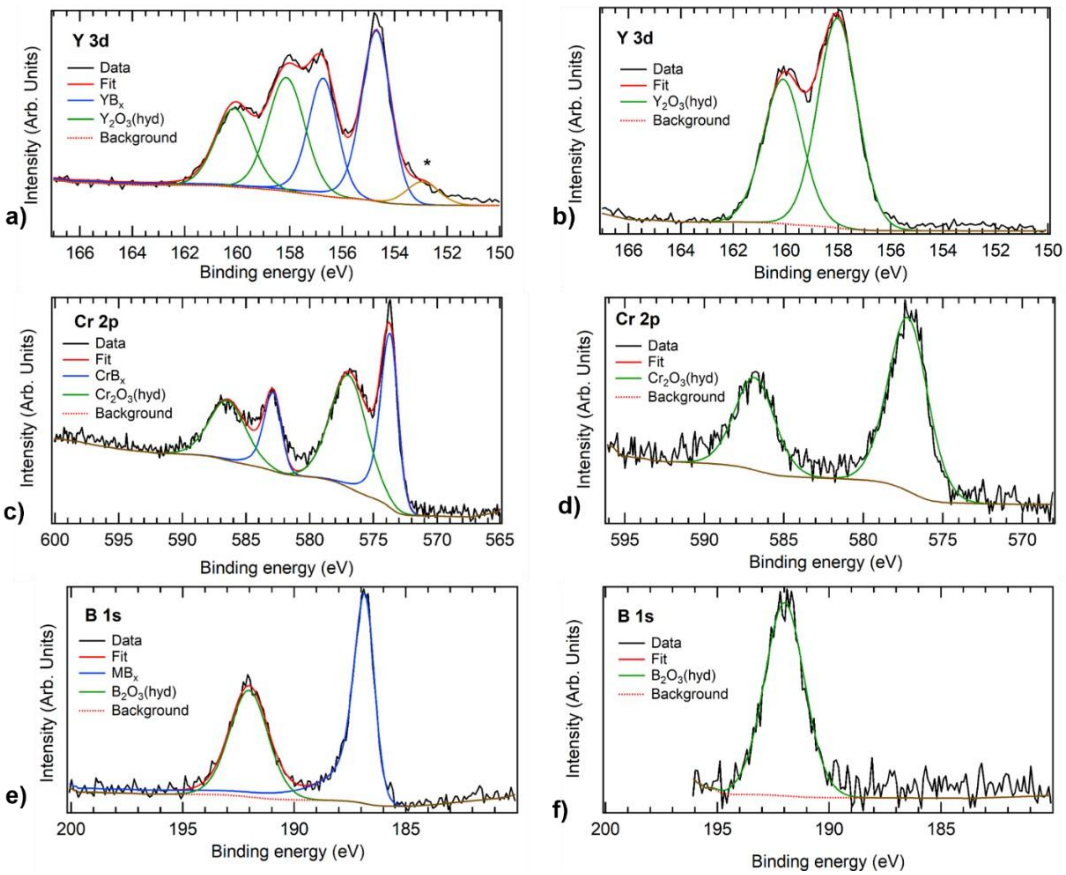


**Figure S5.** XPS core levels spectra for $YCrB_4$ (Y3d, Cr2p, B1s); Before electrocatalysis: a), c), e); After electrocatalysis: b), d), f). The star indicates a Si surface contamination. (Ref S19,20)

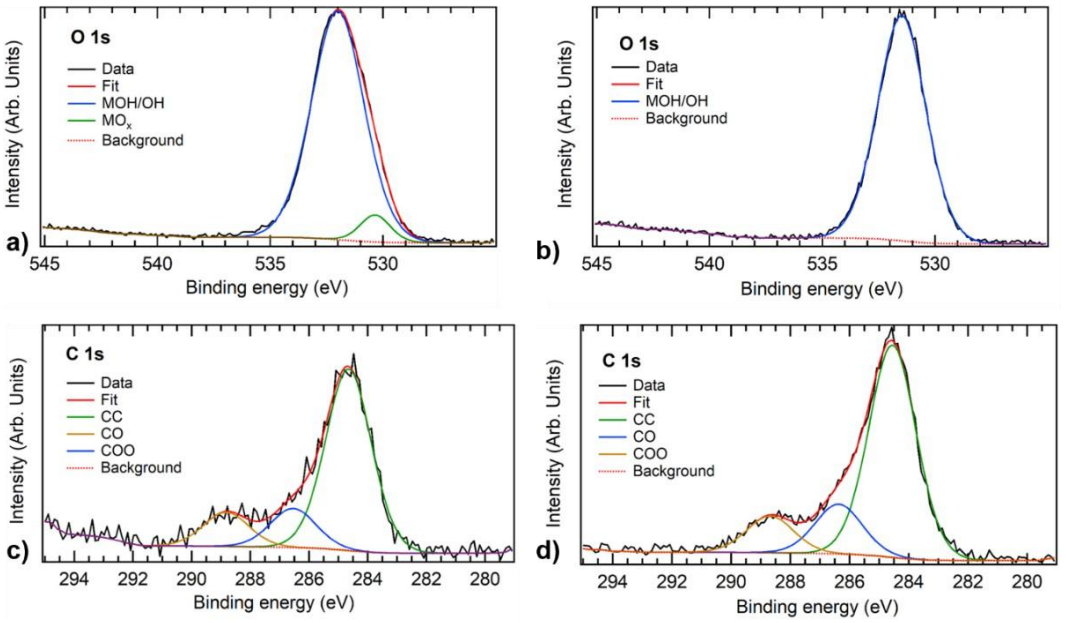


**Figure S6.** XPS core levels spectra for $YCrB_4$ (O1s, B1s); Before electrocatalysis: a), c); After electrocatalysis: b), d).

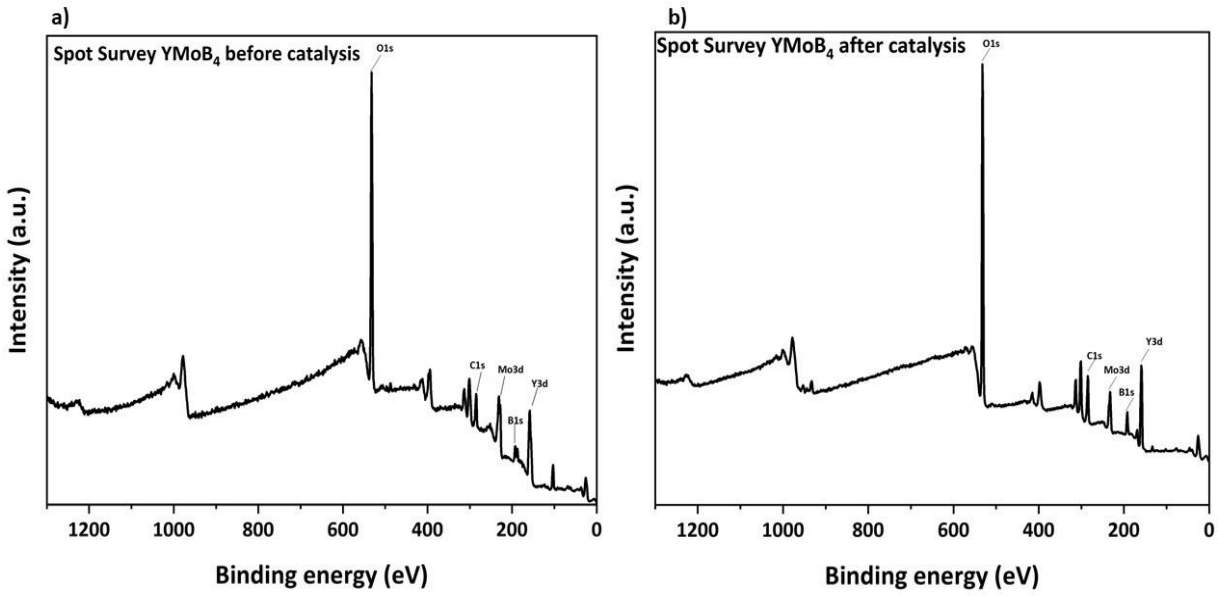


**Figure S7.** XPS survey scan for $YMoB_4$; **a)** before, and **b)** after electrocatalysis.

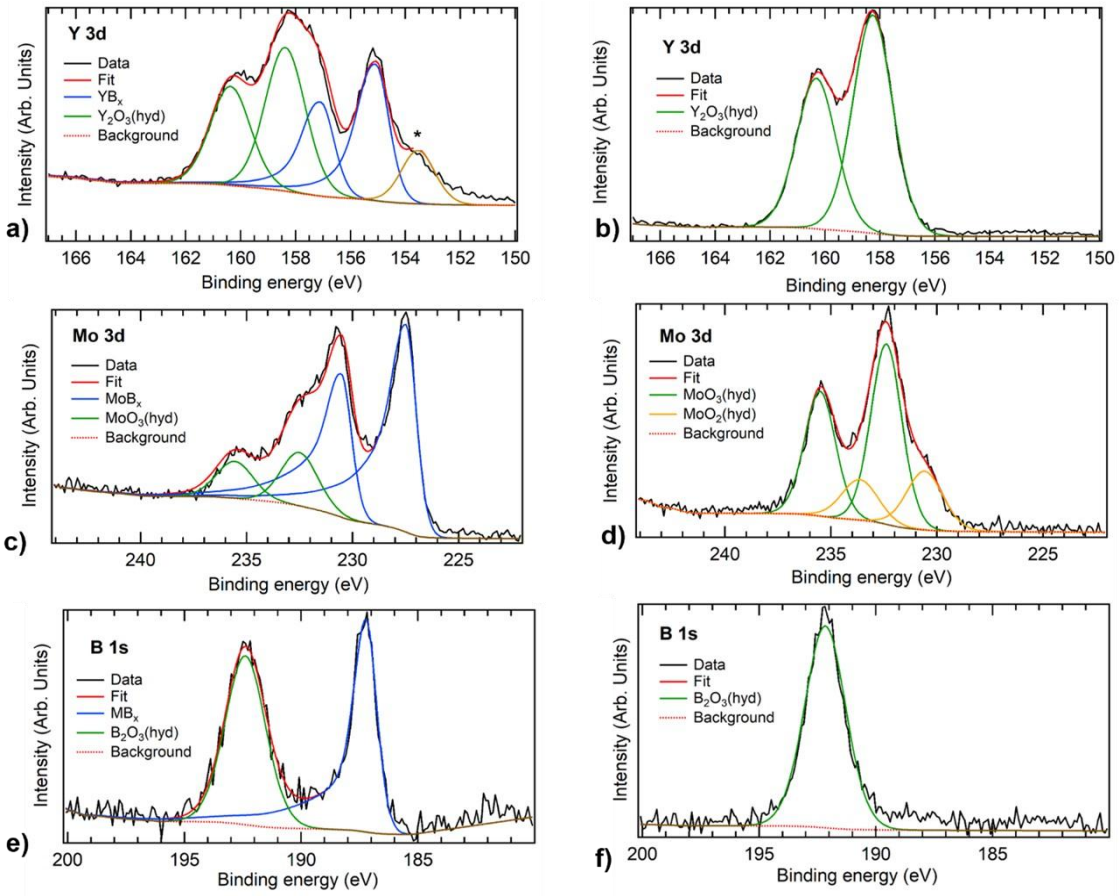


**Figure S8.** XPS core levels spectra for $YMoB_4$ (Y3d, Mo3d, B1s); Before electrocatalysis: a), c), e); After electrocatalysis: b), d), f). The star indicates a Si surface contamination. (Ref S19-22)

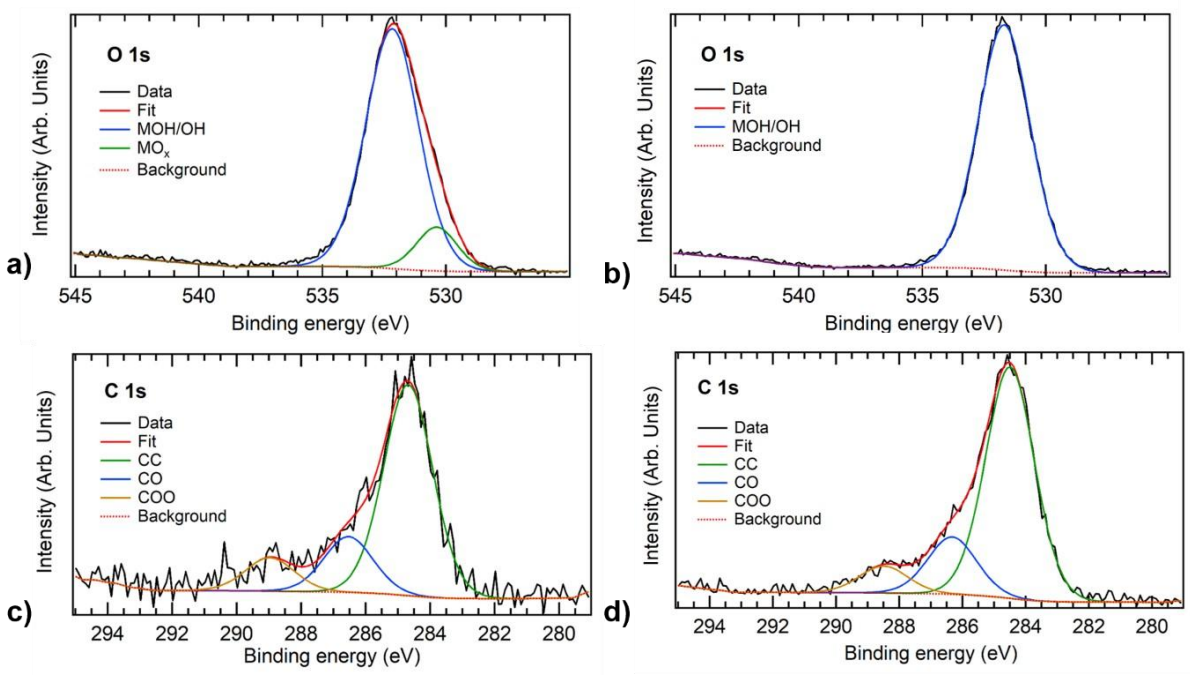


**Figure S9.** XPS core levels spectra for $YMoB_4$ (O1s, B1s); Before electrocatalysis: a), c); After electrocatalysis: b), d).

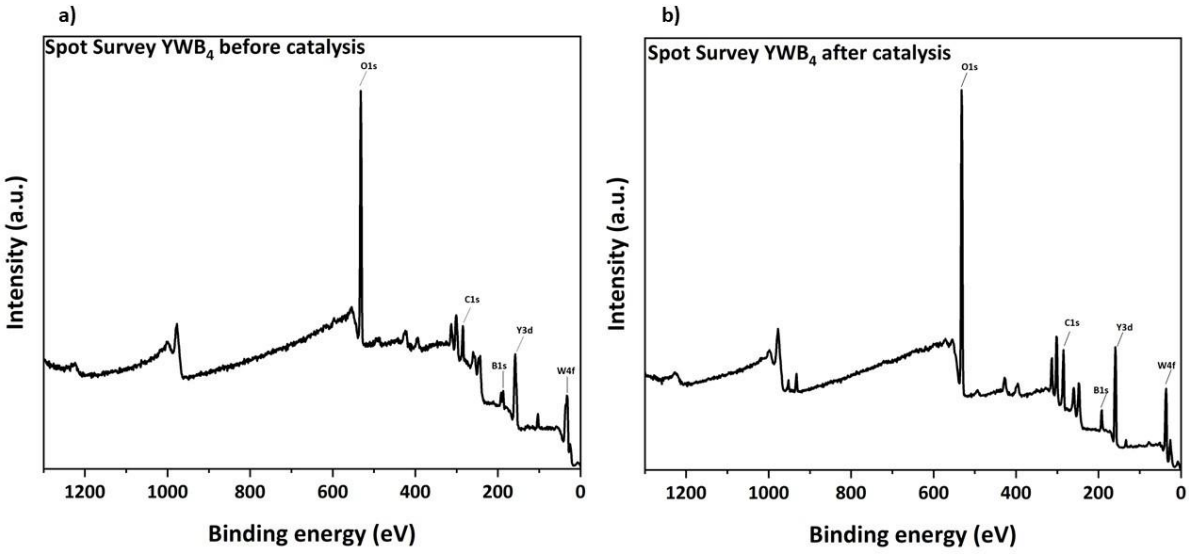


**Figure S10.** XPS survey scan for $YWB_4$; a) Before electrocatalysis, b) After electrocatalysis

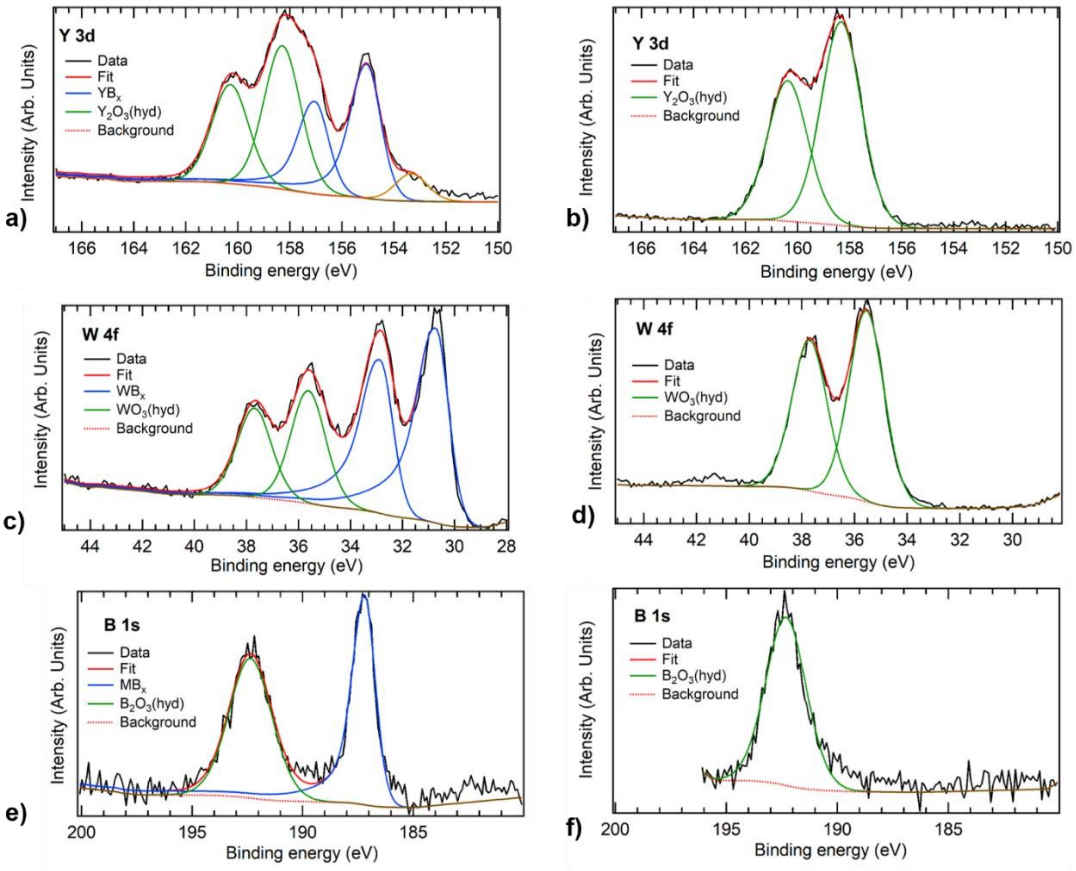


**Figure S11.** XPS core levels spectra for $YWB_4$ (Y3d, W4f, B1s); Before electrocatalysis: a), c), e); After electrocatalysis: b), d), f). The star indicates a Si surface contamination (Ref S19,23)

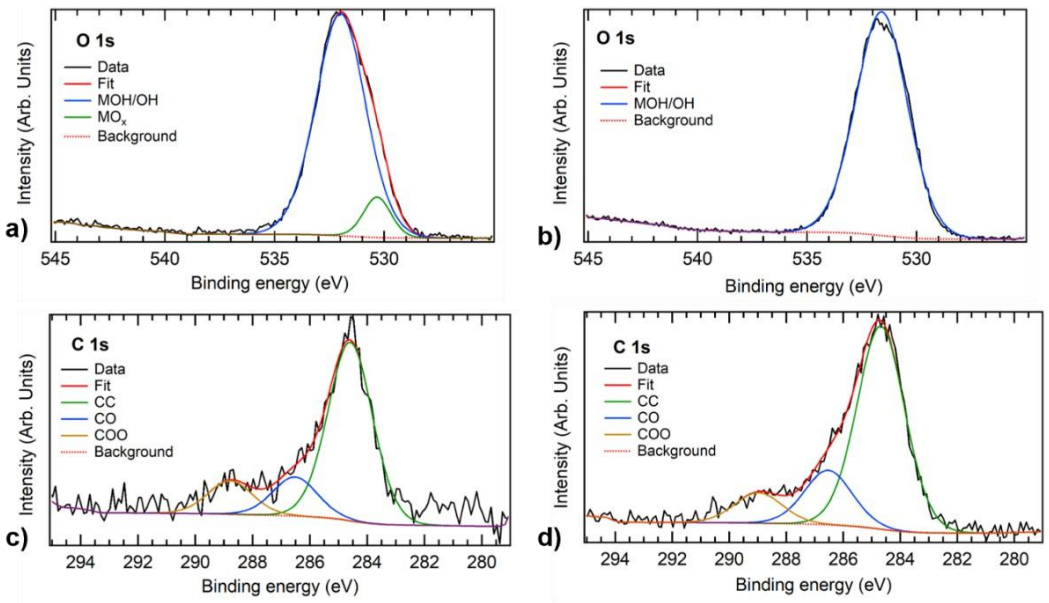


**Figure S12.** XPS core levels spectra for $YWB_4$ (O1s, C1s); Before electrocatalysis: a), c); After electrocatalysis: b), d).

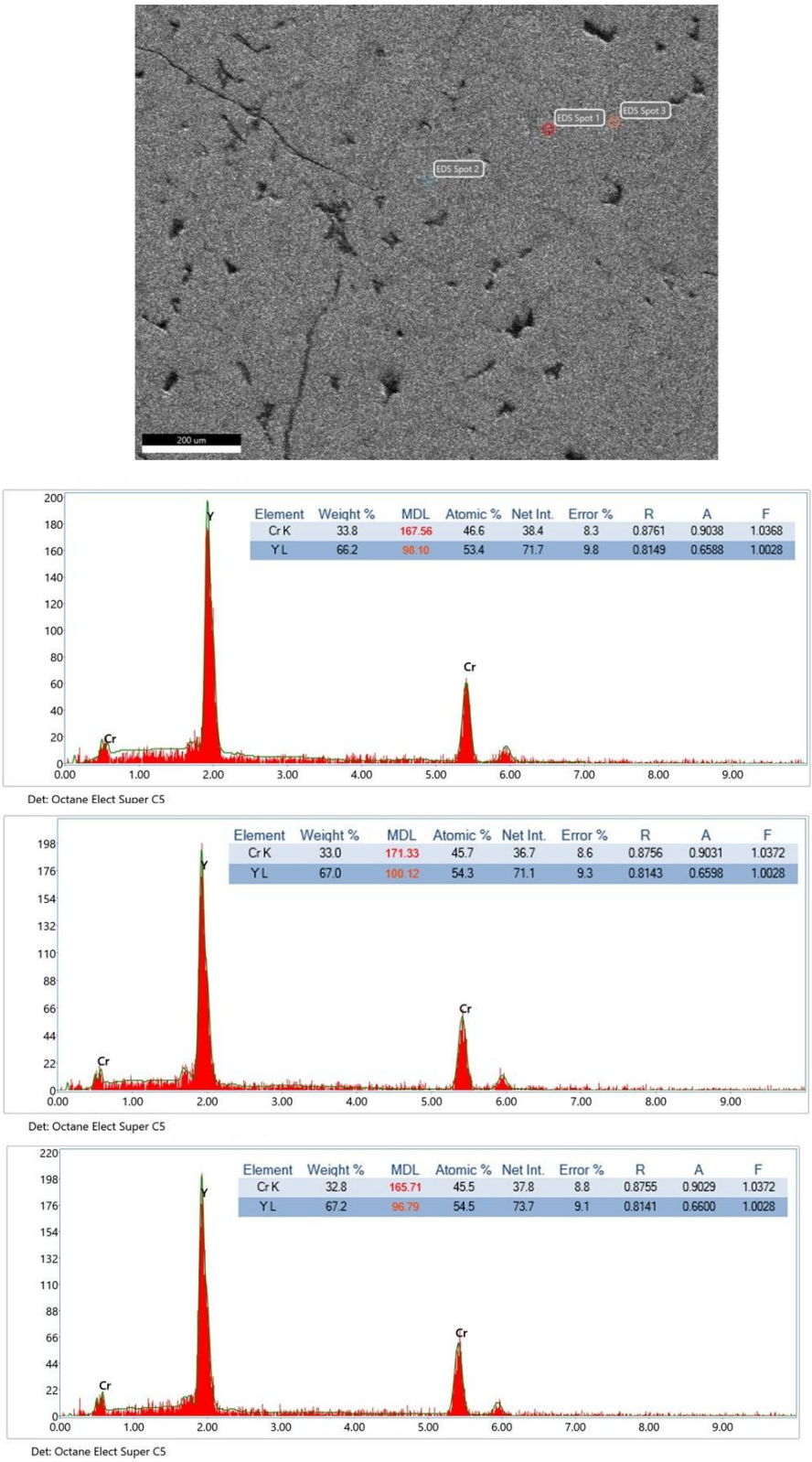


**Figure S13.** SEM-EDS for $YCrB_4$ (Experimental error can be 10 - 20% with relative standard deviation of 1 - 4%.

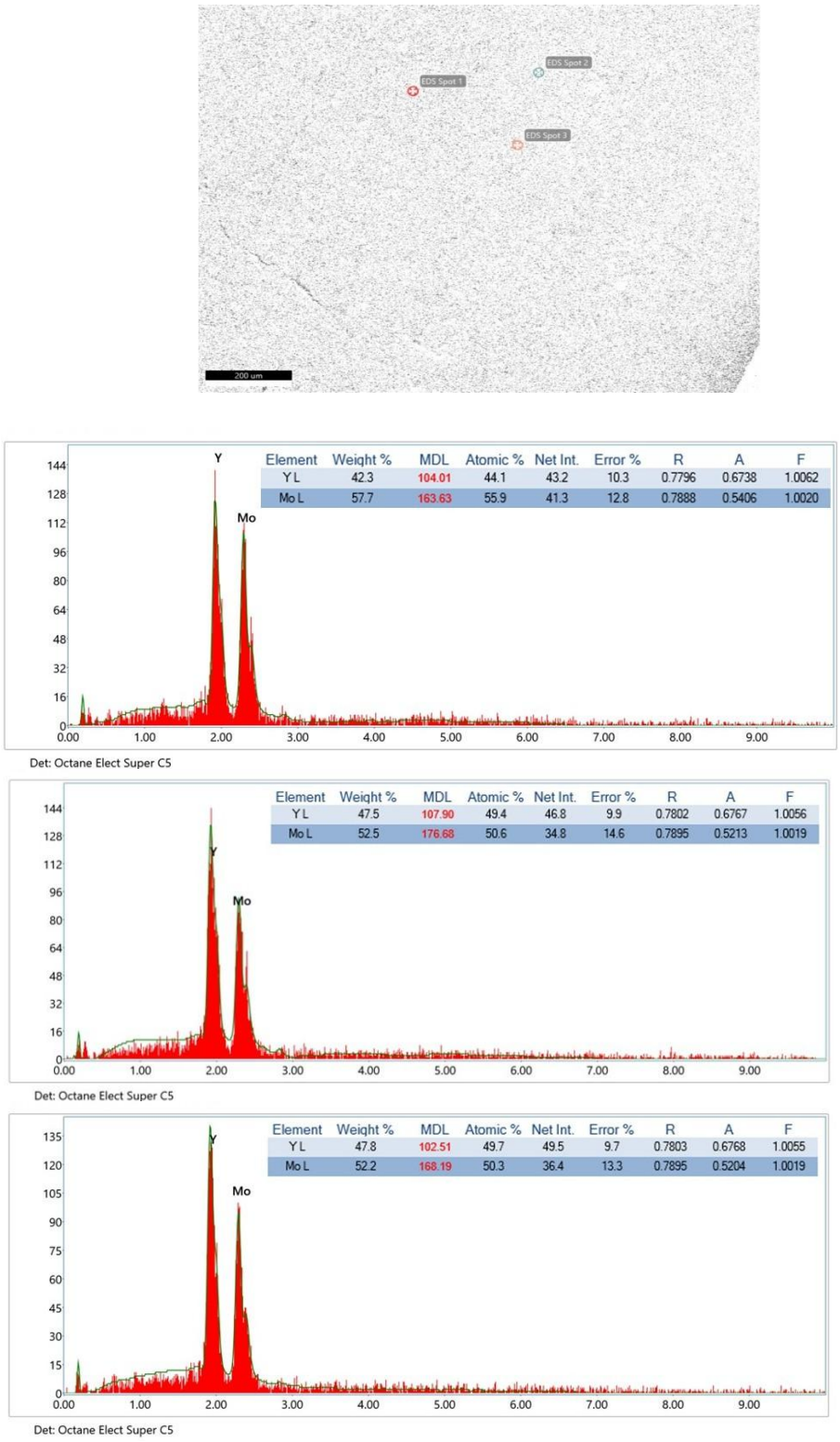


**Figure S14.** SEM-EDS for $YMoB_4$ (Experimental error can be 10 - 20% with relative standard deviation of 1-4%).

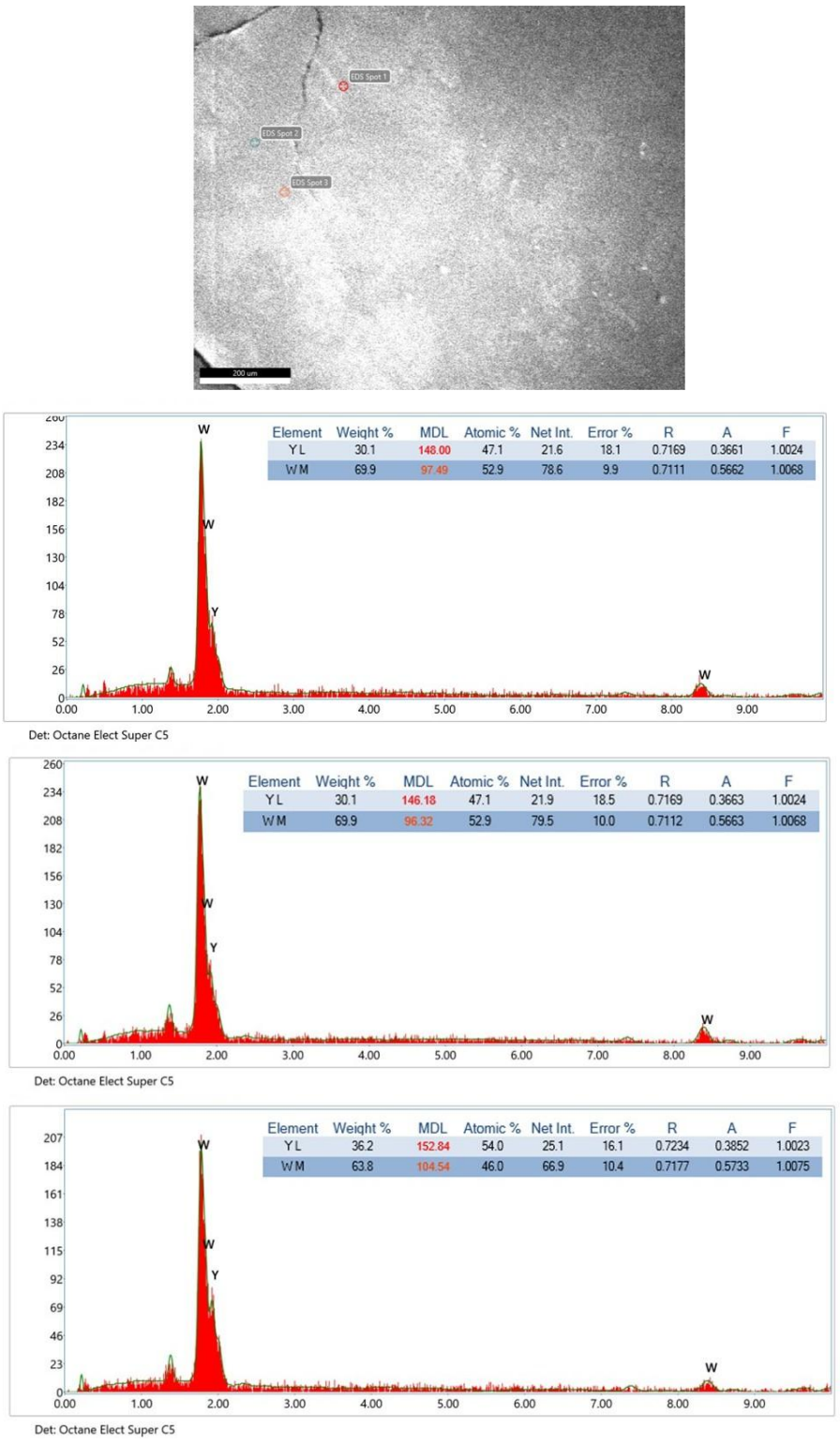


**Figure S15.** SEM-EDS for $YWB_4$ (Experimental error can be 10 - 20% with relative standard deviation of 1-4%).

## References


1. Park, H.; Lee, E.; Lei, M.; Joo, H.; Coh, S.; Fokwa, B. P. T. Advanced Materials 2020, 32 (28), 2000855.
2. Kim, S. B.; Yapo, J. A.; Yasuhara, A.; Yubuta, K.; Fokwa, B. P. T. Small, 2412693.
3. Xiao, P.; Sk, M. A.; Thia, L.; Ge, X.; Lim, R. J.; Wang, J.-Y.; Lim, K. H.; Wang, X. Energy Environ. Sci. 2014, 7 (8), 2624–2629.
4. Zhu, L., Lin, H., Li, Y. et al. Nat Commun 7, 12272 (2016).
5. Park, H.; Encinas, A.; Scheifers, J. P.; Zhang, Y.; Fokwa, B. P. T. Angewandte Chemie International Edition 2017, 56 (20), 5575–5578.
6. Vrubel, H.; Hu, X. Angewandte Chemie International Edition 2012, 51 (51), 12703–12706.
7. Jothi, P. R.; Zhang, Y.; Scheifers, J. P.; Park, H.; Fokwa, B. P. T. Sustainable Energy Fuels 2017, 1 (9), 1928–1934.
8. Park, H.; Zhang, Y.; Scheifers, J. P.; Jothi, P. R.; Encinas, A.; Fokwa, B. P. T. J Am Chem Soc 2017, 139 (37), 12915–12918
9. Alameda, L. T.; Holder, C. F.; Fenton, J. L.; Schaak, R. E. Chem. Mater. 2017, 29 (21), 8953–8957
10. Kibsgaard, J., Chen, Z., Reinecke, B. et al. Nature Mater 11, 963–969 (2012).
11. Chen, W.-F.; Wang, C.-H.; Sasaki, K.; Marinkovic, N.; Xu, W.; Muckerman, J. T.; Zhu, Y.; Adzic, R. R. Energy Environ. Sci. 2013, 6 (3), 943–951
12. Yanli Chen, Guangtao Yu, Wei Chen, Yipu Liu, Guo-Dong Li, Pinwen Zhu, Qiang Tao, Qiuju Li, Jingwei Liu, Xiaopeng Shen, Hui Li, Xuri Huang, Dejun Wang, Tewodros Asefa, and Xiaoxin Zou. Journal of the American Chemical Society 2017 139 (36), 12370-12373
13. Voiry, D., Yamaguchi, H., Li, J. et al. Nature Mater 12, 850–855 (2013).
14. McEnaney, J. M.; Chance Crompton, J.; Callejas, J. F.; Popczun, E. J.; Read, C. G.; Lewis, N. S.; Schaak, R. E. Chem. Commun. 2014, 50 (75), 11026–11028.
15. Wirth, S.; Harnisch, F.; Weinmann, M.; Schröder, U. Appl. Catal. B: Environ. 2012, 126, 225–230.
16. Gupta, S.; Patel, N.; Miotello, A.; Kothari, D. C. Journal of Power Sources 2015, 279, 620–625.
17. Chen, Z.; Kang, Q.; Cao, G.; Xu, N.; Dai, H.; Wang, P. International Journal of Hydrogen Energy 2018, 43 (12), 6076–6087.
18. Li, H.; Wen, P.; Li, Q.; Dun, C.; Xing, J.; Lu, C.; Adhikari, S.; Jiang, L.; Carroll, D. L.; Geyer, S. M. Adv. Energy Mater. 2023, 13 (21), 2300489.
19. Brown, R.; Vorokhta, M.; Skála, T.; Khalakhan, I.; Lindahl, N.; Eriksson, B.; Lagergren, C.; Matolínová, I.; Matolín, V.; Wickman, B. Fuel Cells 2020, 20 (4), 413–419.
20. Mavel, G.; Escard. J.; Costa P.; Castaing J., Surf. Sci. **1973**, 35, 109-116
21. Natu, V.; Kota, S. S.; Barsoum, M. W. *J. Eur. Ceram. Soc.* **2020**, *40* (1), 305–314
22. Vrubel, H.; Hu, X. *Angew. Chem., Int. Ed.* **2012**, *51* (51), 12703–12706.
23. Choi, J.-G.; Thompson, L. T. *Appl. Surf. Sci.* **1996**, *93* (2), 143–149.

24. Zhang, X.; Luo, H.; Wang, Y.; Li, K.; Wen, H.; Bu, W.; Liu, B.; Yan, K. *Chemical Engineering Science* **2025**, *318*, 122199.